Analysis of the Enol Ether Transfer Catalyzed by UDP-GlcNAc Enolpyruvyl Transferase Using (*E*)- and (*Z*)-Isomers of Phosphoenolbutyrate: Stereochemical, Partitioning, and Isotope Effect Studies

Watson J. Lees and Christopher T. Walsh*

Contribution from the Department of Biological Chemistry and Molecular Pharmacology, Harvard Medical School, Boston, Massachusetts 02115

Received March 7, 1995[⊗]

Abstract: Both (*E*)- and (*Z*)-phosphoenolbutyrates (PEB) were substrates for UDP-GlcNAc enolpyruvyl transferase, MurZ, the first enzyme of bacterial cell wall biosynthesis, and were converted to a mixture of (*E*)- and (*Z*)-enolbutyryl-UDP-GlcNAc (EB-UDP-GlcNAc). The catalytic rates for both isomers of PEB were about 0.2% that of the natural substrate, phosphoenolpyruvate (PEP). The initial kinetic ratio of (*E*)- to (*Z*)-enol ether products, 13:1, was similar for both (*E*)- and (*Z*)-PEB. The enzyme was thus stereoselective for the formation of the (*E*)-enol ether product but not stereospecific. On the other hand, the equilibrium ratio of (*E*)- to (*Z*)-enol ether products was 1:35; the thermodynamic product, (*Z*)-EB-UDP-GlcNAc, was different from the kinetic product, (*E*)-EB-UDP-GlcNAc. The overall equilibrium constant between (*Z*)-PEB and UDP-GlcNAc and (*Z*)-enol ether product and phosphate was approximately 65. (*E*)-PEB was also converted under initial velocity conditions to (*Z*)-PEB in addition to enol ether products, reflecting partitioning from an intermediate. In contrast, (*Z*)-PEB was not converted to a detectable amount of (*E*)-PEB. In D_2O, (*E*)-[^{1}H]PEB was transformed to (*Z*)-[^{2}H]enol ether product and (*E*)-[^{1}H]enol ether product. Therefore, we concluded that the enzyme catalyzes either a *syn*-addition of UDP-GlcNAc to PEB and an *anti*-elimination of phosphate from an intermediate or an *anti*-addition and a *syn*-elimination. This is similar to the paired stereochemical alternatives in the reaction catalyzed by 5-enolpyruvylshikimate-3-phosphate synthase (EPSP synthase).

Introduction

The first committed step in bacterial cell wall biosynthesis, a transfer of an enolpyruvyl group from phosphoenolpyruvate (PEP) to uridine 5′-diphospho-*N*-acetylglucosamine (UDP-GlcNAc), is catalyzed by MurZ (EC 2.5.1.7, UDP-*N*-acetylglucosamine enolpyruvyl transferase) (Scheme 1).[1] The enol ether product of this reaction, enolpyruvyl-UDP-GlcNAc (EP-UDP-GlcNAc), is converted by a multienzyme pathway to an activated peptidoglycan unit, uridine 5′-diphospho-*N*-acetylmuramic acid with a pentapeptide side chain (UDP-MurNAc-pentapeptide). This activated peptidoglycan is then glycosylated with UDP-GlcNAc to form a disaccharyl pentapeptide unit which is transported across the cell membrane and polymerized to generate the bacterial cell wall. The cell wall protects the organism against osmotic shock and is essential for survival. MurZ is a potential site for the action of antibiotics and indeed is inactivated by the antibacterial drug fosfomycin (also called phosphomycin and phosphonomycin), an epoxyphosphonate analog of PEP that covalently modifies the enzyme.[2-4]

To elucidate the mechanism of enol ether formation by MurZ, we and others have been investigating PEP,[5-9] (*E*)- and (*Z*)-3-fluorophosphoenolpyruvate (FPEP),[10,11] and fosfomycin[2-4] as substrates and inhibitors of MurZ. Using the physiological substrates PEP and UDP-GlcNAc, we demonstrated that the reaction catalyzed by MurZ involves two kinetically-competent intermediates.[5] One intermediate is a covalently bound phospholactyl–enzyme adduct, **1** (Scheme 2), and the other intermediate is a noncovalently bound phospholactyl-UDP-GlcNAc tetrahedral ketal, **2**. The rate-determining step was determined to be the breakdown of **2**. The kinetic data obtained using the natural substrates did not indicate whether **2** could be formed directly without the prior formation of **1**. This issue was addressed using the fluorinated analog FPEP. We determined that MurZ reacted with FPEP to produce a noncovalently bound fluorinated tetrahedral intermediate, F-**2**, and a fluorinated enzyme-bound adduct, F-**1**.[10,11] Neither enzyme-bound F-**1** nor F-**2** undergoes breakdown in the forward direction to form fluorinated EP-UDP-GlcNAc. We also showed that F-**2** could be formed directly from (*Z*)-FPEP, UDP-GlcNAc, and MurZ without the prior formation of F-**1**. By analogy, we proposed that the natural substrate PEP follows a similar direct pathway to **2** as in Scheme 2. The rate constant for the formation of F-**2**, which contains a strongly electron withdrawing fluoro substituent, was less, by a factor of 10^4, than the rate constant for the formation of **2**. The inability of F-**1** or F-**2** to break down in the forward direction reflects a retardation in rate of at

[⊗] Abstract published in *Advance ACS Abstracts*, June 15, 1995.

(1) Park, J. T. In *Escherichia Coli and Salmonella Typhimurium: Cellular and Molecular Biology*; Neidhardt, F. C., Ingraham, J. L., Low, K. B., Magasanik, B., Schaechter, M., Umbarger, H. E., Eds.; American Society for Microbiology: Washington, DC, 1987; Vol. 1, pp 663–671.

(2) Kahan, F. M.; Kahan, J. S.; Cassidy, P. J.; Kropp, H. *Ann. N. Y. Acad. Sci.* **1974**, *235*, 364–386.

(3) Wanke, C.; Amrhein, N. *Eur. J. Biochem* .**1993**, *218*, 861–870.

(4) Marquardt, J. L.; Brown, E. D.; Lane, W. S.; Haley, T. M.; Ichikawa, Y.; Wong, C. H.; Walsh, C. T. *Biochemistry* **1994**, *33*, 10646–10651.

(5) Brown, E. D.; Marquardt, J. L.; Lee, J. P.; Walsh, C. T.; Anderson, K. S. *Biochemistry* **1994**, *33*, 10638–10645.

(6) Marquardt, J. L.; Brown, E. D.; Walsh, C. T.; Anderson, K. S. *J. Am. Chem. Soc.* **1993**, *115*, 10398–10399.

(7) Ramilo, C.; Appleyard, R. J.; Wanke, C.; Krekel, F.; Amrhein, N.; Evans, J. N. S. *Biochemistry* **1994**, *33*, 15071–15079.

(8) Zemell, R. I.; Anwar, R. A. *J. Biol. Chem.* **1975**, *250*, 4959–4964.

(9) Cassidy, P. J.; Kahan, F. M. *Biochemistry* **1973**, *12*, 1364–1374.

(10) Kim, D. H.; Lees, W. J.; Walsh, C. T. *J. Am. Chem. Soc.* **1994**, *116*, 6478–6479.

(11) Kim, D. H.; Lees, W. J.; Haley, T. M.; Walsh, C. T. *J. Am. Chem. Soc.* **1995**, *117*, 1494–1502.

0002-7863/95/1517-7329$09.00/0

Scheme 1. Initial Steps of Peptidogycan Assembly

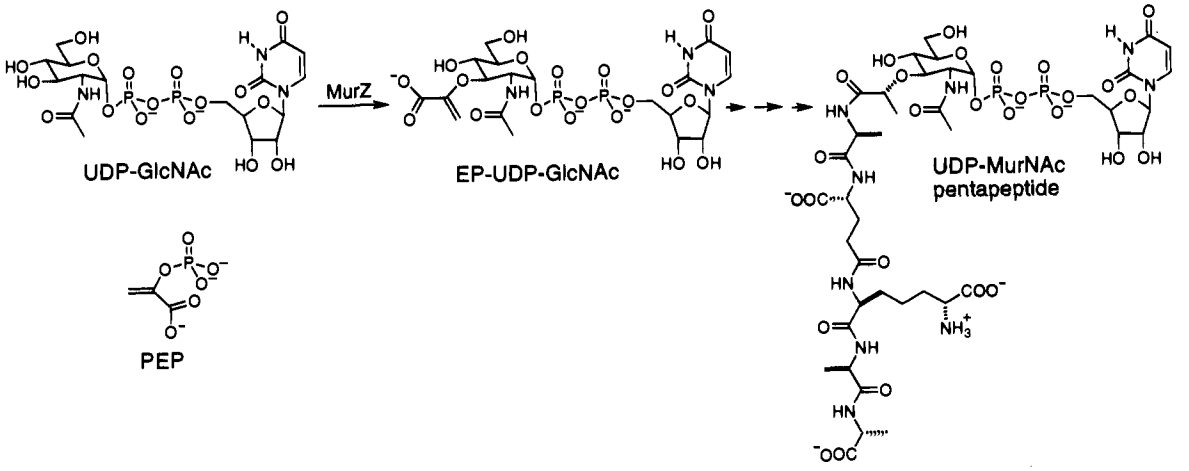

Scheme 2. Proposed Mechanism of MurZ

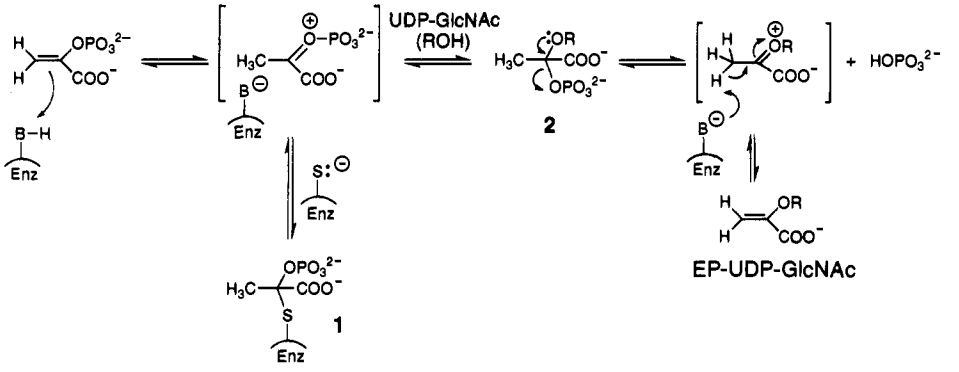

least 10^6 compared to the breakdown of **2**. These results strongly suggested that the transition states for the formation and breakdown of **2** by MurZ contain a large amount of oxocarbenium ion character (Scheme 2). **1** is proposed to be covalently attached to the enzyme through Cys-115.[2-4] We and others have shown that Cys-115 is essential for catalysis and that the antibiotic fosfomycin irreversibly inhibits MurZ by alkylating Cys-115.

Studies of the mechanism of MurZ have been partially directed by previous mechanistic work on 5-enolpyruvylshikimate-3-phosphate synthase (EPSP synthase), the only other enzyme known to catalyze the transfer of an enolpyruvyl group from PEP.[12,13] The mechanism of EPSP synthase is similar to that proposed for MurZ in that EPSP synthase also proceeds through a non-covalently bound ketal tetrahedral intermediate.[14-16] EPSP synthase also reacts slowly with (*Z*)-FPEP to form a fluorinated, non-covalently bound tetrahedral intermediate that does not decompose to product.[17-19] However, unlike MurZ, no covalent enzyme-bound adduct has been detected for EPSP synthase.

Substrate analogs of PEP have been useful for studying the mechanism of other PEP-utilizing enzymes. (*Z*)- and/or (*E*)-phosphoenolbutyrates (PEB) have previously been shown to be inhibitors for prolidase,[20] enolase,[21-23] phosphoenolpyruvate carboxykinase,[22,24] and deoxyarabinoheptulosonate synthase,[25] and substrates for phosphoenolpyruvate carboxylase,[26-29] pyruvate kinase,[21,22,30-35] phosphotransferase system I,[36] and MurZ.[8] (*Z*)-PEB has been used previously as a mechanistic probe to determine the stereochemistry of the addition of hydrogen to

(12) Levin, J. G.; Sprinson, D. B. *J. Biol. Chem.* **1964**, *239*, 1142-1150.
(13) Bondinell, W. E.; Vnek, J.; Knowles, P. F.; Sprecher, M.; Sprinson, D. B. *J. Biol. Chem.* **1971**, *246*, 6191-6196.
(14) Anderson, K. S.; Sikorski, J. A.; Johnson, K. A. *Biochemistry* **1988**, *27*, 7395-7406.
(15) Anderson, K. S.; Sikorski, J. A.; Benesi, A. J.; Johnson, K. A. *J. Am. Chem. Soc.* **1988**, *110*, 6577-6579.
(16) Anderson, K. S.; Sammons, R. D.; Leo, G. C.; Sikorski, J. A.; Benesi, A. J.; Johnson, K. A. *Biochemistry* **1990**, *29*, 1460-1465.
(17) Walker, M. C.; Ream, J. E.; Sammons, D.; Logusch, E. W.; O'Leary, M. H.; Somerville, R. L.; Sikorski, J. A. *Bioorg. Med. Chem. Lett.* **1991**, *1*, 683-688.
(18) Walker, M. C.; Jones, C. R.; Somerville, R. L.; Sikorski, J. A. *J. Am. Chem. Soc.* **1992**, *114*, 7601-7603.
(19) Seto, C. T.; Bartlett, P. A. *J. Org. Chem.* **1994**, *59*, 7130-7132.
(20) Radzicka, A.; Wolfenden, R. *Biochemistry* **1991**, *30*, 4160-4164.
(21) Duffy, T. H.; Saz, H. J.; Nowak, T. *Biochemistry* **1982**, *21*, 132-139.
(22) Soeling, H. D.; Walter, U.; Sauer, H.; Kleineke, J. *FEBS Lett.* **1971**, *19*, 139-143.
(23) Lane, R. H.; Hurst, J. K. *Biochemistry* **1974**, *13*, 3292-3297.
(24) Duffy, T. H.; Markovitz, P. J.; Chuang, D. T.; Utter, M. F.; Nowak, T. *Proc. Natl. Acad. Sci. U.S.A.* **1981**, *78*, 6680-6683.
(25) Simpson, R. J.; Davidson, B. E. *Eur. J. Biochem.* **1976**, *70*, 501-507.
(26) Gonzalez, D. H.; Andreo, C. S. *Eur. J. Biochem.* **1988**, *173*, 339-343.
(27) Fujita, N.; Izui, K.; Nishino, T.; Katsuki, H. *Biochemistry* **1984**, *23*, 1774-1779.
(28) Izui, K.; Matsuda, Y.; Kameshita, I.; Katsuki, H.; Woods, A. E. *J. Biochem. (Tokyo)* **1983**, *94*, 1789-1795.
(29) Silverstein, R. *Biochim. Biophys. Acta* **1972**, *258*, 626-636.
(30) Woods, A. E.; O'Bryan, J. M.; Mui, P. T. K.; Crowder, R. D. *Biochemistry* **1970**, *9*, 2334-2338.
(31) Bondinell, W. E.; Sprinson, D. B. *Biochem. Biophys. Res. Commun.* **1970**, *40*, 1464-1467.
(32) Stubbe, J. A.; Kenyon, G. L. *Biochemistry* **1971**, *10*, 2669-2677.
(33) Woods, A. E.; Chatman, V. B.; Clark, R. A. *Biochem. Biophys. Res. Commun.* **1972**, *46*, 1-4.
(34) Blumberg, K.; Stubbe, J. *Biochim. Biophys. Acta* **1975**, *384*, 120-126.
(35) Adlersberg, M.; Dayan, J.; Bondinell, W. E.; Sprinson, D. B. *Biochemistry* **1977**, *16*, 4382-4387.
(36) Hoving, H.; Nowak, T.; Robillard, G. T. *Biochemistry* **1983**, *22*, 2832-2838.

C_3 of PEP in the reaction catalyzed by phosphotransferase system I.[36] The product from the MurZ-catalyzed reaction with (*Z*)-PEB in ^3H_2O was previously reported not to incorporate solvent tritium atoms but was incompletely characterized.[8] In this paper, we show that both (*E*)- and (*Z*)-PEBs are processed to (*E*)- and (*Z*)-enolbutyryl ether products by MurZ. We have also determined the relative stereochemistry of the addition and elimination steps and have investigated the incorporation of solvent-derived hydrogens into products.

Experimental Section

General Methods and Materials. Reagents and solvents were reagent grade and used as received. Cyclohexylamine, Br_2, 1,2-dichloroethane, diethyl ether, and diethyl phosphite were obtained from Fluka Chemical Corp. α-Ketobutyrate was obtained from Eastman Chemical Co. (Kodak). Trimethylphosphite (Gold Label) was obtained from Aldrich Chemical Co. Carbon tetrachloride and methanol were obtained from J. T. Baker. Glucose, dithiothreitol (DTT), fosfomycin, and ADP were obtained from Sigma Chemical Co. Hydrogen peroxide (30%) was obtained from Fisher Scientific. Ion-exchange resins AG1-X8 (chloride form, 200−400 mesh) and AG 50W-X8 (hydrogen form, 100−200 mesh) were purchased from Bio-Rad Laboratories. The enolpyruvyl transferase MurZ (EC 2.5.1.7) was purified with 1 equiv of covalently bound PEP as described previously.[5,37] Catalase (EC 1.11.1.6, from bovine liver) and pyruvate kinase (EC 2.7.1.40, from rabbit muscle) were obtained from Sigma Chemical Co. Hexokinase (EC 2.7.1.1, from yeast) was obtained from Boehringer Mannheim Corp.

^1H and ^{13}C NMR spectra were obtained at 400 and 100 MHz, respectively. Proton chemical shifts in D_2O were referenced to HOD set at 4.8 ppm. Carbon chemical shifts in D_2O were referenced to an internal or an external standard of dioxane set at 67.6 ppm. The pH meter reading in D_2O buffer was corrected (pD = pH meter reading + 0.4).

Analytical reversed phase HPLC was performed on a Vydac C_{18} peptide and protein column {1 mL/min, $HCOO^-(NH_4)^+$ [50 mM, pH 4.7] or $CH_3COO^-(NH_4)^+$ [50 mM, pH 4.7]}. The effluent was monitored at 262 nm using a Waters 486 tunable absorbance detector. The retention times for UDP-GlcNAc, (*E*)-EB-UDP-GlcNAc, and (*Z*)-EB-UDPGlcNAc were 4, 5, and 7 min, respectively. Analytical anion-exchange HPLC was performed on a Pharmacia Mono Q column {2 mL/min, $NaHCO_3$ (125 mM for 6 min, then 500 mM for 2 min, then 125 mM for 4 min), pH 9.2}. The effluent was monitored at 235 nm using a Waters 486 tunable absorbance detector. The retention times for (*E*) and (*Z*)-PEB were 3 and 5 min, respectively. The relative extinction coefficients for (*E*)- and (*Z*)-PEB in 125 mM $NaHCO_3$, pH 9.2, were 1.2:1. This was determined by injecting a mixture of (*E*)- and (*Z*)-PEB, whose relative concentration had been determined by ^1H NMR spectroscopy, onto the anion exchange HPLC column. Preparative reversed phase HPLC was performed on a Bio-Rad Hi-pore RP-318 reversed phase HPLC column, and the effluent was monitered at 262 nm.

The reaction rate constants were determined by fitting the data to linear or exponential curves using KaleidaGraph version 3.0.1. The exponential curves were fit to [species] = $c_1(1 - e^{-c_2 t})$, where c_1 and c_2 are variables and t is time. The initial rate was determined by multiplying c_1 by c_2.

Synthesis of (*E*)-Phosphoenolbutyrate. The (*E*)-PEB isomer was synthesized by a modification of the procedure of Duffy et al.[21,30,32,35,38] The fractions obtained from the final purification step, anion-exchange chromatography, were analyzed for both (*E*)-PEB (absorbance at 240 nm) and adenine derivatives (absorbance at 280 nm). Those fractions that did not absorb above background at 280 nm were combined, lyophilized, dissolved in water, and neutralized with 1 N KOH or 1 N NaOH.

Synthesis of (*Z*)-Phosphoenolbutyrate. The (*Z*)-PEB isomer was synthesized by a modification of the procedure of Adlersberg et al.[35,39] The final anion-exchange column was eluted with 0.06 N HCl and then 0.10 N HCl instead of the previously reported 0.02 N HCl and then 0.04 N HCl.[21]

Enzymatic Synthesis of Uridine 5′-(Trihydrogen diphosphate), P′-[2-(Acetylamino)-3-*O*-((*E*)-1-carboxyprop-1-enyl)-2-deoxy-α-D-glucopyranosyl] Ester ((*E*)-EB-UDP-GlcNAc, 3). Aqueous solutions of (*Z*)-PEB (0.25 mL, 200 mM, pH 7.5), UDP-GlcNAc (0.25 mL, 200 mM, pH 7.3), and MurZ (2.0 mL, 0.16 mM in 50 mM aqueous Tris/HCl buffer, pH 8.0) were mixed together. After 6 h, the reaction mixture, which had progressed to 40% completion as determined by analytical reversed phase HPLC, was loaded onto a preparative reversed phase HPLC column and eluted with $HCOO^-(NH_4)^+$ (5 mL/min, 50 mM, pH 4.1). The (*E*)-EB-UDP-GlcNAc, which eluted at 22−32 min, was collected and lyophilized. The resulting powder was lyophilized from water three times to provide 10.3 mg of (*E*)-EB-UDP-GlcNAc (30% yield): ^1H NMR (D_2O) δ 7.94 (d, 1H, H6″, J = 8.1 Hz), 5.97 (d, 1H, H1′, J = 4.3 Hz), 5.95 (d, 1H, H5″, J = 7.9 Hz), 5.63 (q, 1H, vinyl of EB, J = 7.4 Hz), 5.50 (dd, 1H, H1, J = 7.3, 3.3 Hz), 4.35 (m, 2H, H2′, H3′), 4.27 (m, 1H, H4′), 4.23 (ddd, 1H, H5′a, J = 11.7, 4.5, 2.6 Hz), 4.16 (m, 1H, H5′b, H2), 4.02 (t, 1H, H3, J = 10.1 Hz), 3.92 (ddd, 1H, H5, J = 10.1, 4.1, 2.2 Hz), 3.85 (dd, 1H, H6a, J = 12.5, 2.2 Hz), 3.79 (dd, 1H, H6b, J = 12.5, 4.3 Hz), 3.71 (t, 1H, H4, J = 10.0 Hz), 2.03 (s, 3H, Ac), 1.82 (d, 3H, methyl of EB, J = 7.4 Hz); ^{13}C NMR (D_2O) δ 175.6, 171.9, 167.3, 152.9, 150.5, 142.8, 117.5, 103.8, 95.8 (d, J = 6.2 Hz), 89.5, 84.3 (d, J = 8.8 Hz), 82.5, 74.8, 74.0, 70.8, 69.9, 66.1 (d, J = 5.0 Hz), 61.3, 53.9 (d, J = 8.8 Hz), 23.2, 13.2; HRMS (FAB, [M − H]$^-$), (*m/e*) calcd for $C_{21}H_{31}O_{19}N_3P_2$ 690.0949, found 690.0958.

Enzymatic Synthesis of Uridine 5′-(Trihydrogen diphosphate), P′-[2-(Acetylamino)-3-*O*-((*Z*)-1-carboxyprop-1-enyl)-2-deoxy-α-D-glucopyranosyl] Ester ((*Z*)-EB-UDP-GlcNAc, 4). An aqueous solution of (*Z*)-PEB (5 mL, 40 mM, pH 7.6) was mixed with an aqueous solution of UDP-GlcNAc (4 mL, 50 mM, pH 7.3). To this mixture was added MurZ (1.0 mL, 1.4 mM, pH 8.0) in 50 mM aqueous Tris/HCl buffer. After 13 d, more MurZ was added (1.0 mL, 1.3 mM, pH 8.0). After 15 d, the reaction mixture, which had progressed to 60% completion as determined by analytical reversed phase HPLC, was loaded in five equal portions onto a preparative reversed phase HPLC column and eluted with $HCOO^-(NH_4)^+$ (5 mL/min, 50 mM, pH 5.0 (note that the eluent for (*E*)-EB-UDP-GlcNAc was adjusted to pH 4.1)). The (*Z*)-EB-UDP-GlcNAc, which eluted at 23−31 min, was collected and lyophilized. The resulting powder was lyophilized from water three times to provide 75 mg of (*Z*)-EB-UDP-GlcNAc (54% yield): ^1H NMR (D_2O) δ 7.94 (d, 1H, H6″, J = 8.1 Hz), 6.14 (q, 1H, vinyl of EB, J = 7.2 Hz), 5.97 (m, 2H, H1′, H5″), 5.50 (dd, 1H, H1, J = 7.5, 2.8 Hz), 4.35 (m, 2H, H2′, H3′), 4.27 (m, 1H, H4′), 4.24−4.18 (m, 3H, H5′a, H2, H3), 4.16 (ddd, 1H, H5′b, J = 11.8, 5.5, 3.0 Hz) 3.94 (ddd, 1H, H5, J = 10.1, 4.2, 2.1 Hz), 3.87 (dd, 1H, H6a, J = 12.4, 2.1 Hz), 3.80 (dd, 1H, H6b, J = 12.4, 4.4 Hz) 3.77 (dd, 1H, H4, J = 10.2, 8.6 Hz), 2.03 (s, 3H, Ac), 1.68 (d, 3H, methyl of EB, J = 7.2 Hz); ^{13}C NMR (D_2O) δ 175.6, 170.8, 167.3, 152.9, 148.8, 142.7, 122.5, 103.7, 95.3 (d, J = 6.0 Hz), 89.4, 84.3 (d, J = 9.2 Hz), 80.2, 74.7, 74.1, 70.7, 69.9, 66.0 (d, J = 5.1 Hz), 61.3, 54.5 (d, J = 8.2 Hz), 23.2, 11.8; HRMS (FAB, [M − H]$^-$) (*m/e*) calcd for $C_{21}H_{31}O_{19}N_3P_2$ 690.0949, found 690.0948.

Determination of $^{13}C-C=C-^1H$ Coupling Constants in (*E*)- and (*Z*)-PEB, and (*E*)- and (*Z*)-EB-UDP-GlcNAc. For (*E*)- and (*Z*)-PEB and (*E*)- and (*Z*)-EB-UDP-GlcNAc, ^{13}C NMR spectra were acquired with broad band ^1H decoupling and with selective decoupling of the vinylic methyl group. For (*E*)-EB-UDP-GlcNAc, a carbon NMR spectrum with selective decoupling of the vinylic hydrogen was also acquired.

Determination of Forward Reaction Rates in H_2O. MurZ (280 μL of a 0.16 mM solution) was added to 6.72 mL of an aqueous mixture containing (*E*)-or (*Z*)-PEB (1.0 mM),[40] UDP-GlcNAc (1.0 mM), DTT (5.0 mM), and Tris/HCl buffer (50 mM, pH 8.0). Every 30 min for 6 h, two 100 μL aliquots of the main reaction mixture were quenched and analyzed as follows: (1) The first aliquot was added to 100 μL of

(37) Marquardt, J. L.; Siegele, D. A.; Kolter, R.; Walsh, C. T. *J. Bacteriol.* **1992**, *174*, 5748−5752.

(38) Sprinson, D. B.; Chargaff, E. *J. Biol. Chem.* **1946**, *164*. 417−432.

(39) Cramer, F.; Voges, D. *Chem. Ber.* **1959**, *92*, 952−955.

(40) The values of K_m for (*E*)- and (*Z*)-PEB are below 100 μM. The values of K_i for (*E*)- and (*Z*)-PEB are 7 and 90 times the value of K_m for phosphoenolpyruvate (0.2 μM), respectively.

a 0.2 N KOH solution before being diluted with 600 μL of H_2O. This basic solution was then injected onto an analytical reversed phase HPLC column. (2) The second aliquot was added to 11 μL of a 1.0 N KOH solution. Hydrogen peroxide (5 μL, 30%) was then added to oxidize the DTT. This solution was then injected onto an analytical anion HPLC exchange column. Every 1 h from 7 to 12 h and sporadically after 12 h, the reaction mixture was quenched and analyzed as above. At 1 min and at 4 h, an aqueous fosfomycin solution (30 μL, 6 mM) was added to a 1 mL aliquot of the main reaction mixture. The 1 mL fosfomycin/enzyme solution was quenched and analyzed as above 2 h later. The sums of the integrals from the analytical reversed phase HPLC traces corresponding to UDP-GlcNAc, (*E*)-EB-UDP-GlcNAc, and (*Z*)-EB-UDP-GlcNAc were normalized to 1.0 mM.[41] The sums of the integrals from the anion-exchange HPLC traces corresponding to (*E*)- and (*Z*)-PEB were normalized to the concentration of UDP-GlcNAc determined from the analytical reversed phase HPLC trace. The above procedure was done concurrently for (*E*)-PEB and (*Z*)-PEB.

Determination of Forward Reaction Rates in D_2O. MurZ was transferred from H_2O into D_2O using a Centriprep 30 (filtration device, MWCO 30 000, Amicon). The enzyme was concentrated from 5 mL (0.16 mM) to 0.6 mL before being diluted with 20 mL of Tris buffer in D_2O (50 mM Tris/DCl, 5 mM DTT, pD 8.0). The diluted solution was again concentrated to 0.6 mL and diluted with 20 mL of Tris buffer in D_2O. This solution was concentrated to 0.6 mL and used in *all* subsequent experiments. The substrates UDP-GlcNAc (two vials of 14 μmol each), (*E*)-PEB (one vial of 14 μmol), and (*Z*)-PEB (one vial of 14 μmol) were lyophilized to dryness. The pellet in each vial was then dissolved in 200 μL of D_2O. The solutions in each vial were again lyophilized and redissolved in 200 μL of D_2O (70 mM each). These solutions were used in subsequent experiments. Three reaction mixtures were then set up and started concurrently by the addition of enzyme in D_2O (70 μL). The first reaction mixture was composed of (*E*)-PEB in D_2O (100 μL), UDP-GlcNAc in D_2O (100 μL), and Tris buffer in D_2O (6.73 mL, 50 mM Tris/DCl, 5 mM DTT, pD 8.0). The second reaction mixture was the same as the first except that (*Z*)-PEB in D_2O (100 μL) was used instead of (*E*)-PEB in D_2O. The third reaction mixture, which was used to determine enzyme concentration, was the same as the first reaction mixture except that all the substrates and buffers were in H_2O and not D_2O (the added enzyme was in D_2O). Every 30 min from 0 to 6 h, every 60 min from 7 to 9 h, and sporadically from 9 h onward, aliquots from the two reaction mixtures in D_2O were quenched and analyzed using the quenching methods outlined in the previous section. Every 30 min from 0 to 90 min, aliquots from the third reaction mixture were quenched and analyzed. The enzyme concentration in D_2O was determined by comparing the data from the third reaction mixture with the data from the (*E*)-PEB reaction in the previous section.

Determination of Reverse Reaction Rates in H_2O. MurZ (800 μL, 0.16 mM) was mixed with UDP-GlcNAc (80 μL, 3 mM) and incubated for 1 h at 25 °C to remove enzyme-bound PEP. The enzyme solution (308 μL) was added to 6.69 mL of an aqueous mixture containing (*E*)- or (*Z*)-EB-UDP-GlcNAc (1.0 mM), potassium phosphate (20 mM, pH 8.0), DTT (5.0 mM), and Tris/HCl buffer (50 mM, pH 8.0). As a control, the same enzyme solution (88 μL) was also added to 1.91 mL of a mixture containing (*E*)-PEB (1 mM), UDP-GlcNAc (1 mM), DTT (5.0 mM), and Tris/HCl buffer (50 mM, pH 8.0). All three reaction mixtures were started concurrently. The reaction mixtures were quenched in the same manner and at the same time points as in the section describing the determination of the forward reaction rates in H_2O. The sums of the integrals from the analytical reversed phase HPLC traces corresponding to UDP-GlcNAc, (*E*)-EB-UDP-GlcNAc, and (*Z*)-EB-UDP-GlcNAc were normalized to 1.0 mM.[41] The sums of the integrals from the anion-exchange HPLC traces corresponding to (*E*)- and (*Z*)-PEB were normalized to the concentration of UDP-GlcNAc determined from the analytical reversed phase HPLC trace (for the reverse reactions the concentration of UDP-GlcNAc was adjusted by the initial concentration of UDP-GlcNAc at $t = 0$). The above procedure was done concurrently for (*E*)-and (*Z*)-EB-UDP-GlcNAc and the control.

(41) The sum of the integrals of the peak areas from the reversed phase HPLC traces are constant with reaction time.

Determination of Equilibrium Constants. After 100 h, the concentration of (*Z*)-PEB in the reaction mixtures initiated with (*E*)- or (*Z*)-PEB or (*E*)- or (*Z*)-EB-UDP-GlcNAc was determined by anion-exchange HPLC, using an internal standard of UDP-GlcNAc or (*E*)-PEB. For the reactions initiated with (*E*)- or (*Z*)-PEB, the concentration of phosphate in the reaction mixtures at 100 h was the difference between the initial concentration of PEB (1 mM) and the determined final concentration of (*Z*)-PEB. For the reactions initiated with (*E*)- or (*Z*)-EB-UDP-GlcNAc, the concentration of phosphate in the reaction mixtures at 100 h was the initial concentration of phosphate (20 mM) less the determined final concentration of (*Z*)-PEB. The sum of the concentrations of UDP-GlcNAc and (*E*)- and (*Z*)-EB-UDP-GlcNAc was assumed to be constant throughout the reaction (1 mM).[41] Their relative concentrations were determined at 100 h by integration of the HPLC chromatogram. Filtration of the reaction mixtures through a Centricon 30, to remove enzyme-bound species prior to quenching at 100 h, did not significantly alter the equilibrium constants.

Determination of the Deuterium Content of EB-UDP-GlcNAc Products Isolated from Reactions Performed in D_2O. Enzyme (1 μmol in 1000 μL), UDP-GlcNAc (two vials of 50 μmol in 250 μL), (*E*)-PEB (50 μmol in 250 μL), and (*Z*)-PEB (50 μmol in 250 μL) in D_2O were prepared as in the section describing the determination of reaction rates in D_2O. Two reaction mixtures were prepared. The first reaction mixture consisted of UDP-GlcNAc (250 μL), (*E*)-PEB (250 μL), enzyme (400 μL, approximately 1.0 mM), and Tris buffer (1600 μL, 50 mM Tris/DCl, pD 8.0) in D_2O. The second reaction mixture was the same as the first except that (*Z*)-PEB (250 μL) replaced (*E*)-PEB. The first reaction mixture was quenched with 0.5 mL of 1 N KOH after 2 h (8% conversion as determined by analytical reversed phase HPLC); the two EB-UDP-GlcNAc products were purified by preparative reversed phase HPLC chromatography (5 mL/min, $HCOO^-(NH_4)^+$, 50 mM, pH 5.0). The second reaction mixture was quenched with 0.5 mL of 1 N KOH after 90 min (7% conversion); the two EB-UDP-GlcNAc products were purified by preparative reversed phase HPLC chromatography as above. Each of the four products was lyophilized from water three times and analyzed by FAB-LRMS and NMR.

Results

Preparation of (*E*)- and (*Z*)-PEB Isomers. (*E*)- and (*Z*)-PEB were synthesized according to published procedures with minor modifications.[21,30,32,35,38,39] In both syntheses, β-bromo-α-ketobutyrate, which was prepared by the addition of bromine to α-ketobutyrate, was used as an intermediate. To synthesize (*E*)-PEB, β-bromo-α-ketobutyrate was converted to dimethyl phosphoenolbutyrate by the addition of trimethyl phosphite in a Perkow reaction. Base hydrolysis of the phosphate methyl esters followed by photoisomerization resulted in a 1:1.5 mixture of (*E*)- and (*Z*)-PEB. The (*Z*)-PEB was selectively removed from the mixture with pyruvate kinase, and the remaining (*E*)-PEB was purified by anion-exchange chromatography. To synthesize (*Z*)-PEB, diethyl phosphite was added to β-bromo-α-ketobutyrate to produce diethyl (1-hydroxy-1-carboxy-2-bromopropyl)phosphonate. The phosphonate was converted to (*Z*)-PEB by the addition of sodium hydroxide solution. The (*Z*)-PEB was purified by precipitating the cyclohexylammonium salt.

Enzymatic Synthesis and Characterization of (*E*)- and (*Z*)-Enolbutyryl-UDPGlcNAc Products. Both (*E*)- and (*Z*)-PEB were active as substrates of MurZ, and in the presence of UDP-GlcNAc, each was converted to a mixture of two isomeric products, (*E*)- and (*Z*)-enolbutyryl-UDP-GlcNAc (EB-UDP-GlcNAc, **3** and **4**, respectively). By controlling the reaction time, we were able to obtain both isomers in 10−100 mg quantities (Scheme 3). Short incubation times (6 h) resulted in the accumulation of (*E*)-EB-UDP-GlcNAc as the major product, whereas longer incubation times (2 weeks) led to the formation of (*Z*)-EB-UDP-GlcNAc. Both isomers were purified by

Scheme 3. Synthesis of (*E*)- and (*Z*)-EB-UDP-GlcNAc

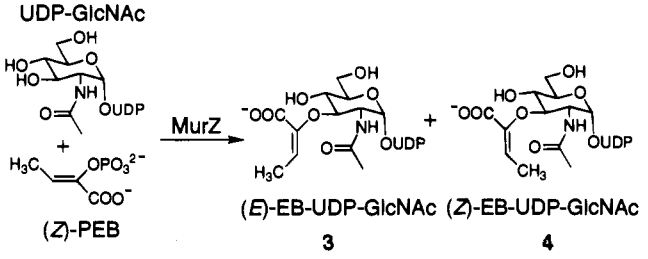

Table 1. $^1H-^{13}C$ Coupling Constants of (*E*)- and (*Z*)-PEB and the Kinetic and Thermodynamic Products

compound	structure	J_{HC} (Hz)	J_{PC} (Hz)
(*E*)-PEB	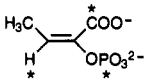	9.0	5.8
(*Z*)-PEB	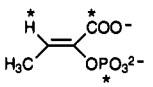	<3[a]	<3[b]
kinetic product	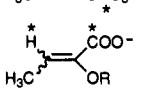	8.4	
thermodynamic product	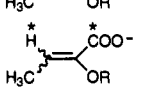	<3[c]	

[a] A splitting of 1.8 Hz was measured in two of four acquired spectra. No splitting was observed in the other two spectra. The digital resolution of the spectra was 0.6 Hz. [b] No splitting was observed in three acquired spectra. The digital resolution of the spectra was 0.6 Hz. [c] A splitting of 2.4 Hz was measured in one of two acquired spectra. No splitting was observed in the other spectrum. The digital resolution of the spectra was 0.6 Hz.

reversed phase HPLC. The two products were characterized by NMR and HRMS.

At the time of the initial purification of the two EB-UDP-GlcNAc product isomers, the stereochemistry about their enolbutyrate double bond was unassigned. By comparing the known $^1H-^{13}C$ coupling constant (vinyl ^1H to $^{13}COOH$) of each PEB isomer with the same $^1H-^{13}C$ coupling constant of the EB-UDP-GlcNAc products, we assigned the stereochemistry of the EB-UDP-GlcNAc products (Table 1). The product isolated after 6 h was the (*E*)-isomer, and the product isolated after 2 weeks was the (*Z*)-isomer.

Catalytic Rates from PEB and EB-UDP-GlcNAc Incubations with MurZ in H_2O and D_2O. The rate constants for the enzymatic conversion of PEB to EB-UDP-GlcNAc products were determined for both PEB isomers in H_2O and D_2O by monitoring the distribution of starting materials and products with reversed phase and anion-exchange HPLC as a function of time (Figures 1 and 2, Table 2). Both (*E*)- and (*Z*)-PEB were converted to (*E*)- and (*Z*)-EB-UDP-GlcNAc. (*E*)-PEB was converted to products 1.7 times faster than (*Z*)-PEB and 350 times slower than the natural substrate PEP (Table 2). For reactions initiated with (*E*)- or (*Z*)-PEB, the initial ratio of (*E*)- to (*Z*)-enol ether product was greater than 10:1, indicating that the (*E*)-enol ether product is the kinetic product (Figure 2). After 100 h, the (*Z*)-enol ether product predominated over the (*E*)-enol ether product in a 35:1 ratio, indicating that the (*Z*)-enol ether product is the thermodynamic product (Figure 1). The interplay of kinetics and thermodynamics results in an initial sharp increase in the concentration of (*E*)-enol ether product followed by a slow decrease in its concentration as a function of reaction time (Figure 1). When (*E*)-PEB was used as a substrate, initial accumulation of (*Z*)-PEB was observed, along with the formation of (*E*)- and (*Z*)-UDP-GlcNAc products. Thus, (*Z*)-PEB presumably resulted from enzyme-catalyzed isomerization of (*E*)-PEB. However, when the reaction was initiated with (*Z*)-PEB, no significant accumulation of (*E*)-PEB was detected. The initial rate at which (*E*)-PEB was isomerized to (*Z*)-PEB was 7 times faster than the initial rate at which (*E*)-PEB was converted to (*Z*)-enol ether product and half the initial rate at which (*E*)-PEB was converted to (*E*)-enol ether product (Figure 2). After 300 min, all of the (*E*)-PEB had been converted to (*Z*)-PEB or EB-UDP-GlcNAc products (Figure 2).

For the reactions initiated with (*E*)-PEB, the product distribution in D_2O was different than that in H_2O. For the reactions

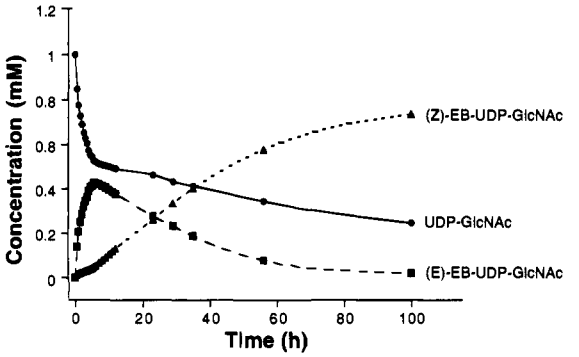

Figure 1. Time course of the reaction of (*E*)-PEB and UDP-GlcNAc. A reaction mixture consisting of MurZ (6.4 μM), (*E*)-PEB (1 mM), and UDP-GlcNAc (1 mM) was quenched at the indicated times, and the concentrations of the species were determined by reversed phase and anion-exchange HPLC (see the Experimental Section). The data points were not fitted to a kinetic model. The time course of the reaction of (*Z*)-PEB and UDP-GlcNAc is included in the supporting information.

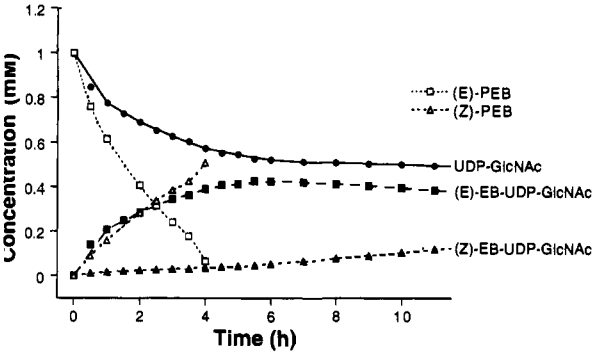

Figure 2. Early time course of the reaction of (*E*)-PEB and UDP-GlcNAc. A reaction mixture consisting of MurZ (6.4 μM), (*E*)-PEB (1 mM), and UDP-GlcNAc (1 mM) was quenched at the indicated times, and the concentrations of the species were determined by reversed phase and anion-exchange HPLC (see the Experimental Section). The data points were not fitted to a kinetic model. The early time course of the reaction of (*Z*)-PEB and UDP-GlcNAc is included in the supporting information.

Table 2. Rate Constants for the MurZ-Catalyzed Reaction between PEB and UDP-GlcNAc

reactant	rate constant (k_{cat})	H_2O (min^{-1})	D_2O (min^{-1})	k_{H_2O}/k_{D_2O}
(*E*)-PEB	$k_{(Z)\text{-PEB}}$[a]	0.42	0.86	0.49
	$k_{(E)\text{-EB-UDP-GlcNAc}}$[a]	0.75	0.39	1.9
	$k_{(Z)\text{-EB-UDP-GlcNAc}}$[a,c]	0.062	0.084	0.74
	$k_{(Z)\text{-EB-UDP-GlcNAc}}$[b,d]	0.033	0.037	0.89
(*Z*)-PEB	$k_{(E)\text{-EB-UDP-GlcNAc}}$[a]	0.45	0.24	1.9
	$k_{(Z)\text{-EB-UDP-GlcNAc}}$[b]	0.031	0.024	1.3

[a] The data were fit to an exponential curve. [b] The data were fit to a linear curve. [c] The initial enzymatic rate in the presence of (*E*)-PEB. [d] The enzymatic rate after greater than 90% of the (*E*)-PEB had been converted to (*Z*)-PEB and EB-UDP-GlcNAc.

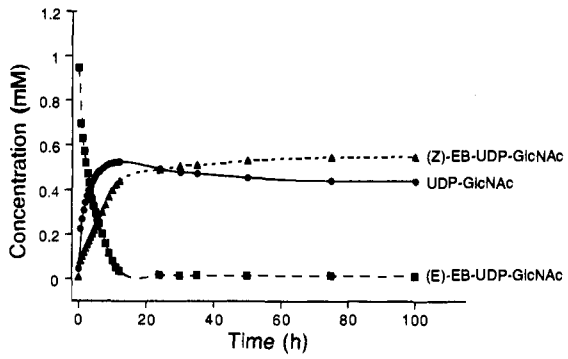

Figure 3. Time course of the reaction of (*E*)-EB-UDP-GlcNAc and phosphate. A reaction mixture consisting of MurZ (6.4 μM), (*E*)-EB-UDP-GlcNAc (1 mM), and phosphate (20 mM) was quenched at the indicated times, and the concentrations of the species were determined by reversed phase and anion-exchange HPLC (see the Experimental Section). The data points were not fitted to a kinetic model. The time course of the reaction of (*Z*)-EB-UDP-GlcNAc and phosphate is included in the supporting information.

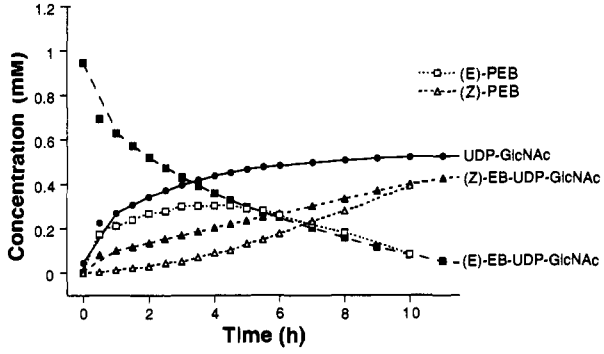

Figure 4. Early time course of the reaction of (*E*)-EB-UDP-GlcNAc and phosphate. A reaction mixture consisting of MurZ (6.4 μM), (*E*)-EB-UDP-GlcNAc (1 mM), and phosphate (20 mM) was quenched at the indicated times, and the concentrations of the species were determined by reversed phase and anion-exchange HPLC (see the Experimental Section). The data points were not fitted to a kinetic model. The time course of the reaction of (*Z*)-EB-UDP-GlcNAc and phosphate is included in the supporting information.

initiated in D_2O, the ratio of the rate constants for the formation of (*E*)-EB-UDP-GlcNAc and (*Z*)-EB-UDP-GlcNAc was 4.6 instead of 12 as in H_2O. The major kinetic route was also changed from the conversion of (*E*)-PEB to (*E*)-enol ether product to the isomerization of (*E*)-PEB to (*Z*)-PEB (Table 2). For the reactions initiated with (*Z*)-PEB, the ratio of the rate constants for the formation of products in D_2O, 10, was similar to that in H_2O, 14.

Kinetics of the Reverse Reaction: Enolether to PEB. The reactions initiated with (*E*)- or (*Z*)-EB-UDP-GlcNAc and phosphate were followed in a manner similar to that of the reactions initiated with PEB (Figures 3 and 4). With (*E*)-EB-UDP-GlcNAc, the concentration of products as a function of time did not fit an exponential or linear function. The ratio of (*E*)- to (*Z*)-PEB products at early time points was approximately 20:1, and the ratio of total PEB to (*Z*)-enol ether was 2.2:1. The time course for the formation of (*E*)-PEB was fit to an exponential function with a value of k_{cat} of 1.1 min^{-1}. The time course for the formation of (*Z*)-PEB was fit to a line for the first 3 h with a value of k_{cat} of 0.05 min^{-1}. The rate of formation of (*Z*)-PEB increased considerably after this initial phase as more (*E*)-PEB accumulated and was converted to (*Z*)-PEB. The time course for the formation of the isomeric enol ether (*Z*)-EB-UDP-GlcNAc had a large initial burst but became linear after 30 min with a value of k_{cat} of 0.08 min^{-1}.[42] With (*Z*)-EB-UDP-GlcNAc as substrate, only a small amount of (*E*)-PEB (<5%) or (*E*)-EB-UDP-GlcNAc (<3%) was generated due to the unfavorable thermodynamics for (*E*)-isomer formation. The early time course for the formation of (*Z*)-PEB was linear with a value of k_{cat} of 0.04 min^{-1}.

Table 3. Equilibrium Ratios for the MurZ-Catalyzed Conversion of (*Z*)-PEB and UDP-GlcNAc to (*E*)-EB-UDP-GlcNAc (**3**), (*Z*)-EB-UDP-GlcNAc (**4**), and Inorganic Phosphate (P_i)

		equilibrium ratios	
starting materials[b]	[**4**]:[**3**]	[(*Z*)-PEB]:[(*E*)-PEB][a]	[**4**][P_i]:[UDP-GlcNAc][(*Z*)-PEB]
(*E*)-PEB + UDP-GlcNAc	33	>6	40
(*Z*)-PEB + UDP-GlcNAc	33	>6	40
3 + P_i	41	>16	80
4 + P_i	44	>17	100

[a] The ratios were determined from the relative integrals of the (*Z*)-PEB peak to the noise in the (*E*)-PEB region of the HPLC trace from the anion-exchange HPLC column. [b] The initial concentrations of (*E*)- or (*Z*)-PEB and UDP-GlcNAc were 1 mM. The initial concentration of **3** or **4** was 1 mM and the initial concentration of phosphate was 20 mM.

Table 4. Relative Mass Spectral Intensities and Approximate Deuterium Content of EB-UDP-GlcNAc Products[a]

		relative intensities[b]			approx
product	reaction	M − 1	M	M + 1	% D
(*E*)-EB-UDP-GlcNAc	perprotio standard	2.8	100	29.4	0
	(*E*)-PEB reactn in D_2O	2.85	100	30.8	1
	(*Z*)-PEB reactn in D_2O	3.9	8.6	100	92
(*Z*)-EB-UDP-GlcNAc	perprotio standard	4.8	100	33.0	0
	(*E*)-PEB reactn in D_2O	3.4	4.6	100	96
	(*Z*)-PEB reactn in D_2O	3.8	11.9	100	86

[a] The reaction conditions are described in the Experimental Section. [b] The mass was determined by negative ion FAB-MS, and M corresponds to the [(molecular mass) − H]$^-$ peak at 690 amu. The highest intensity peak was assigned a value of 100.

The thermodynamic parameters of the MurZ-catalyzed conversion of (*E*)- and (*Z*)-PEB to (*E*)- and (*Z*)-EB-UDP-GlcNAc products and vice versa were also determined by allowing each of the four reactions to approach equilibrium after 4 d (Table 3). The thermodynamic product ratio of (*E*)- to (*Z*)-EB-UDP-GlcNAc, 1:37, was very different and inverted from the initial product ratio of 13:1 (Figures 1 and 2). The thermodynamics of the reaction also favored the formation of (*Z*)-enol ether product and phosphate over (*Z*)-PEB and UDP-GlcNAc by 65:1.

In order to determine the relative stereochemistry of the addition and elimination reactions catalyzed by MurZ, the initial EB-UDP-GlcNAc products (from reactions carried out in D_2O to less than 10% conversion) were purified by reversed phase HPLC and analyzed by FAB-LRMS (Table 4). The (*E*)-EB-UDP-GlcNAc product from the (*E*)-PEB reaction fully retained a proton at C_3, but the (*Z*)-EB-UDP-GlcNAc product from this reaction was fully deuterated at C_3. Surprisingly, both (*E*)- and (*Z*)-EB-UDP-GlcNAc products from the (*Z*)-PEB reaction were deuterated at C_3 of their enolbutyryl groups. The mechanistic implications of these results will be discussed below.

(42) The absolute values of k_{cat}, but not the relative values, were also somewhat dependent on enzyme concentration as a 10-fold decrease in enzyme concentration resulted in a-20 fold decrease in rate and a 2-fold decrease in the values of k_{cat}.

Scheme 4. Stereoselective but Not Stereospecific Reaction with a Common Reaction Intermediate

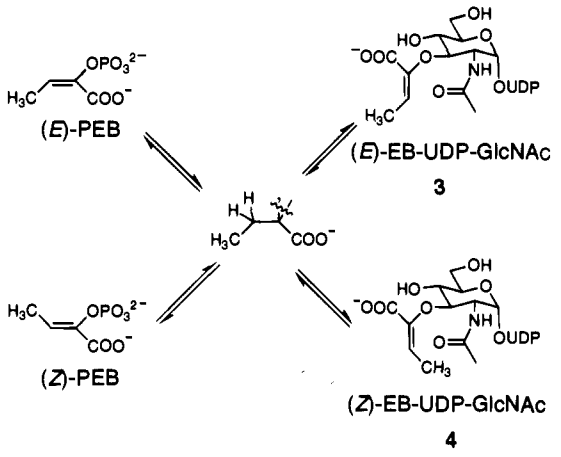

Discussion

MurZ-Catalyzed Reaction of PEB and UDP-GlcNAc in H_2O. MurZ catalyzes the conversion of both substrate isomers (*E*)- and (*Z*)-PEB to a mixture of two products, (*E*)-EB-UDP-GlcNAc and (*Z*)-EB-UDP-GlcNAc (Scheme 3), and equilibrates the kinetic product(*E*)-EB-UDP-GlcNAc with the thermodynamic product (*Z*)-EB-UDP-GlcNAc. The catalytic rate constants for MurZ with (*E*)- and (*Z*)-PEB, 0.8 and 0.5 min^{-1}, are 350- and 600-fold slower, respectively, than the catalytic rate constant for MurZ with the natural substrate PEP.[40] The slower rates may be a result of the greater steric hindrance of the methyl group of PEB as compared with the hydrogen of PEP. However, the position of the methyl group around the double bond of PEB, *cis* or *trans* to the phosphate, affects the catalytic rate only slightly. The two reaction products were characterized by mass spectroscopy and NMR. The stereochemistry about their enolbutyryl double bonds was assigned by measuring the $^1H-^{13}C$ coupling constant between the vinylic hydrogen and the carbonyl carbon (Table 1).

The assignment of the stereochemistry of the two products allows the reaction manifold to be analyzed. The initial kinetic ratio of (*E*)- to (*Z*)-EB-UDP-GlcNAc products is similar for both (*E*)- and (*Z*)-PEB, 12:1 and 14:1, respectively, with the (*E*)-EB-UDP-GlcNAc product predominating. The reaction is thus stereoselective but not stereospecific. Since the kinetic product ratio is similar regardless of the double bond stereochemistry of the starting material, a common intermediate is likely. We therefore interpret the mechanism in terms of Scheme 4, with an intermediate diagramed here as an sp^3 methylene locus at C_3 formed by protonation of the PEB double bond. (The substitution at C_2, i.e., ketal, covalent enzyme thioether, or oxocarbenium ion, is not specified at this point.) At long reaction times the (*E*) to (*Z*) product ratio inverts with the (*Z*)-UDP-GlcNAc product predominating over the (*E*)-UDP-GlcNAc product in a 35:1 ratio. Thus, the (*Z*)-enol ether product is the thermodynamic product, and MurZ catalyzes the interconversion between (*E*)- and (*Z*)-enol ether products.

The back reaction starting from both (*E*)- and (*Z*)-enol ether products can be analyzed in a manner similar to that of the forward reaction. In the back-reaction the initial kinetic ratio of (*E*)- to (*Z*)-PEB products was 20:1 from (*E*)-EB-UDP-GlcNAc, with the (*E*)-PEB predominating. With (*Z*)-EB-UDP-GlcNAc the highest observed concentration of (*E*)-PEB was 50 μM. This is presumably due to the relative thermodynamic stabilities of (*Z*)-EB-UDP-GlcNAc and (*E*)-PEB. Therefore, it was difficult to determine the initial kinetic ratio of (*E*)- to (*Z*)-PEB, but (*E*)-PEB was the predominant species. As observed in the forward reaction, the back-reaction is stereoselective but not stereospecific and conforms to the mechanism in Scheme 4. The thermodynamic ratio of (*E*)- to (*Z*)-PEB was determined to lie on the side of (*Z*)-PEB with a greater than 10:1 ratio. Again in the back-direction, the kinetic product (*E*)-PEB is different from the thermodynamic product (*Z*)-PEB and MurZ catalyzes their interconversion. These data describe the overall thermodynamics of the reaction depicted in Scheme 5.

Scheme 5. Thermodynamics of the MurZ-Catalyzed Conversion of PEB to EB-UDP-GlcNAc

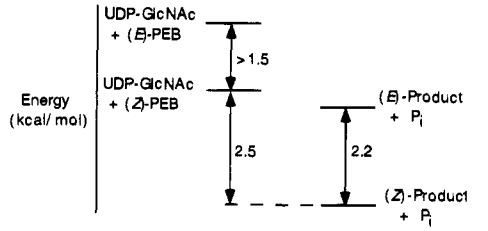

In the forward reaction we observe that MurZ isomerizes (*E*)-PEB to (*Z*)-PEB in competition with (*E*)- and (*Z*)-enol ether product formation. We do not observe the converse of this result; (*E*)-PEB is not observed to accumulate during the reaction of (*Z*)-PEB to (*E*)- and (*Z*)-enol ether products. The partitioning of (*E*)-PEB to both products and also to (*Z*)-PEB again supports a mechanism similar to Scheme 4 in which an intermediate can partition either in the forward or backward direction. The absence of an observable amount of (*E*)-PEB during the reaction of (*Z*)-PEB to both products may be a result of two factors: (1) the greater thermodynamic stability of (*Z*)-PEB over (*E*)-PEB (>10:1) under the reaction conditions as indicated by Scheme 5; (2) the rate of (*Z*) to (*E*) isomerization may be slower than that of (*E*)-PEB to (*E*)- or (*Z*)-EB-UDP-GlcNAc conversion.

In the back-reaction a similar result is obtained. (*E*)-EB-UDP-GlcNAc is likewise converted to the isomeric (*Z*)-EB-UDP-GlcNAc in competition with (*E*)- and (*Z*)-PEB formation. (*Z*)-EB-UDP-GlcNAc is converted to (*E*)-EB-UDP-GlcNAc in competition with (*E*)- and (*Z*)-PEB formation, but the observed concentration of (*E*)-EB-UDP-GlcNAc is never greater than the thermodynamic ratio of 1:35 ((*E*)-EB-UDP-GlcNAc:(*Z*)-EB-UDP-GlcNAc).

MurZ-Catalyzed Reaction of PEB and UDP-GlcNAc in D_2O. We investigated the overall reaction rate, the product distribution, and the deuterium content of the products for reactions run in D_2O. The overall reaction rate for the formation of products from (*E*)-PEB in D_2O was 1.7-fold slower than the corresponding reaction rate in H_2O. The kinetic partitioning in D_2O was considerably different from that in H_2O due to an apparent "inverse isotope effect" for the formation of (*Z*)-EB-UDP-GlcNAc and (*Z*)-PEB from (*E*)-PEB. In H_2O, the ratio of the rates for the formation of (*Z*)-PEB, (*E*)-EB-UDP-GlcNAc, and (*Z*)-EB-UDP-GlcNAc was 6.8:12:1, but in D_2O, the ratio was 10:4.6:1, respectively. This change in the ratio of rates is most likely a result of an internal competition for a deuterium or hydrogen atom on the now deuterated intermediates, Scheme 6 (from D^+ addition to C_3 of the double bond of PEB). Since the relative rate of formation of (*E*)-enol ether product is slower in D_2O than in H_2O, we would expect that the (*E*)-enol ether product is formed in D_2O by the loss of a deuterium atom which is kinetically less favorable than the loss of a proton. The (*Z*)-enol ether product (and also the partitioning back to (*Z*)-PEB) would occur by the loss of a proton (Scheme 6). These three predictions imply that the (*E*)-enol ether product should have a vinylic proton on its enolbutyryl group and that the (*Z*)-enol

Scheme 6. Partitioning of the Deuterated Intermediate Generated from (*E*)-PEB in D_2O (Relative Rates Indicated)

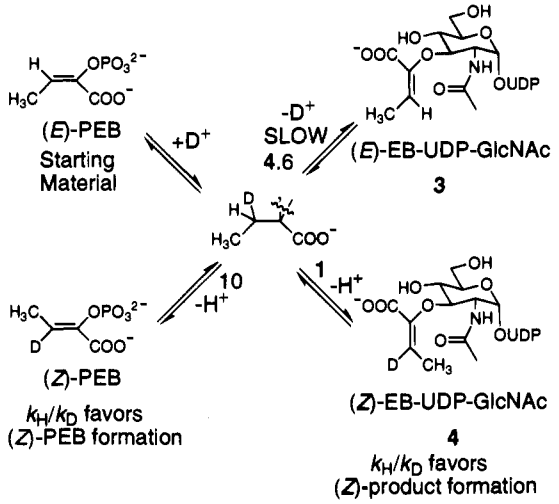

Scheme 7. Generation of Dideuterio Intermediate from (*Z*)-PEB in D_2O

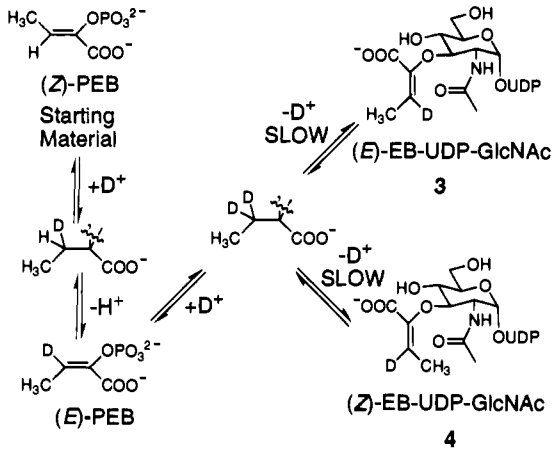

ether product and (*Z*)-PEB should have vinylic deuteriums. All three of these implications are borne out experimentally when both products are isolated, or the reaction is followed *in situ* by ^1H NMR.

For the reaction of (*Z*)-PEB in D_2O, the initial overall reaction rate was slowed by a factor of 1.8 relative to the initial overall rate for the same reaction in H_2O. The kinetic partitioning of products in D_2O was similar to that in H_2O, 10:1 vs 14:1 ((*E*)-EB-UDP-GlcNAc:(*Z*)-EB-UDP-GlcNAc). Surprisingly, both (*E*)- and (*Z*)-enol ether products isolated from the reaction of (*Z*)-PEB in D_2O contained vinylic deuterium atoms on their enolbutyryl groups. Taken together, these results suggest that the (*Z*)-PEB reaction in D_2O involves a dideuterio intermediate, Scheme 7. We propose that the dideuterio intermediate is obtained by (*Z*)-[^{1}H]PEB isomerizing to (*E*)-[^{2}H]PEB and the (*E*)-[^{2}H]PEB being converted to products. The conversion of (*Z*)-[^{1}H]PEB to (*E*)-[^{2}H]PEB is the reverse of converting (*E*)-[^{1}H]PEB to (*Z*)-[^{2}H]PEB in D_2O, which has been demonstrated to occur. Contrary to what we observe, previous work[8] suggests that (*Z*)-PEB is enzymatically converted to nontritiated EB-UDP-GlcNAc in tritiated water. The (*Z*)-PEB used in this earlier work was synthesized by a method that sometimes produces a mixture of (*E*)- and (*Z*)-PEB.[21,31,32,43] Since in this previous work the reaction was run to a low percent conversion, the isolated EB-UDP-GlcNAc may represent EB-UDP-GlcNAc derived from (*E*)-PEB and not (*Z*)-PEB. If this was the case, then these earlier results would be consistent with the results reported herein.

Relative Stereochemistry of Addition and Elimination Steps. The relative stereochemistry of the addition of UDP-GlcNAc to PEB and the elimination of phosphate from the tetrahedral intermediate can be determined from the deuterium content of the products derived from (*E*)-PEB in D_2O. On the basis of the mechanism concluded from previous work with PEP and FPEP (Scheme 2), we conclude either a *syn*-addition of UDP-GlcNAc to PEB and an *anti*-elimination of phosphate from the tetrahedral intermediate or an *anti*-addition and a *syn*-elimination occurs (Scheme 8). To distinguish between these two possibilities, it will be necessary to determine the stereochemistries at C_2 and C_3 of the tetrahedral intermediate derived from a reaction run in D_2O. The stereochemistry of the pair of addition and elimination steps of EPSP synthase were also determind to be either *syn/anti* or *anti/syn*.[44,45] In the case of EPSP synthase, this result was obtained using (*Z*)-[3-$^2H_1$,$^3H_1$]-PEP instead of (*E*)-PEB.[46]

Reaction Mechanism. The proposed reaction mechanism for MurZ with (*E*)-PEB as a substrate, Scheme 9, is based on Scheme 2 and the above results. The covalent enzyme adduct is omitted from Scheme 9 as it is proposed not to be on the direct pathway to product formation but rather to be an adduct into which the first oxocarbenium ion partitions reversibly. PEB and the natural substrate PEP differ by virtue of the methyl group at C_3 of PEB. This methyl group has the potential to cause steric hindrance upon binding of PEB to the enzyme. The additional methyl group may also affect the ability of any intermediate that has an sp^3 carbon at C_3 of its butyryl group to rotate freely about the C_2-C_3 bond. An intermediate with a tetrahedral carbon at C_3, formed from the natural substrate PEP, is torsiosymmetric, with three equivalent methyl hydrogens, whereas an intermediate formed from PEB has two prochiral hydrogens and a bulky methyl group. If none of the intermediates along the reaction pathway for PEB have rotational freedom about their C_2-C_3 bond, then the rotational configuration about the C_2-C_3 bond of the intermediates generated from (*Z*)-PEB will be different from those generated from (*E*)-PEB, assuming that PEB is protonated stereospecifically by the enzyme. These intermediates that differ in their C_2 to C_3 rotational configuration should also partition differently to products. Since (*E*)- and (*Z*)-PEB in fact partition similarly to (*E*)- and (*Z*)-enol ether products at least one of the intermediates along the pathway must rotate about the C_2-C_3 bond. If a single common intermediate along the reaction pathway for PEB has rotational freedom about its C_2-C_3 bond, then the partitioning of (*E*)-PEB to (*Z*)-PEB and (*Z*)-enol ether product should be the same as the partitioning of (*E*)-enol ether product to (*Z*)-PEB and (*Z*)-enol ether product, since each will reach the same intermediate with the same potential for partitioning. The observed result is that (*E*)-PEB and (*E*)-enol ether product partition differently; therefore, we conclude that there must be at least

(43) Dougherty, T. M.; Cleland, W. W. *Biochemistry* **1985**, *24*, 5875–5880.

(44) Lee, J. J.; Asano, Y.; Shieh, T.-L.; Spreafico, F.; Lee, K.; Floss, H. G. *J. Am. Chem. Soc.* **1984**, *106*, 3367–3368.

(45) Grimshaw, C. E.; Sogo, S. G.; Copley, S. D.; Knowles, J. R. *J. Am. Chem. Soc.* **1984**, *106*, 2699–2700.

(46) On the basis of the alternate mechanism for MurZ, in which **1** is required to be formed before **2**, we would predict either an *anti*-addition of enzyme nucleophile to PEB and an *anti*-elimination of phosphate from the tetrahedral intermediate or *syn*-addition and *syn*-elimination. This prediction for the alternate mechanism assumes that the UDP-GlcNAc displaces the enzyme from **1** with inversion of stereochemistry.

(47) The face of attack of UDP-GlcNAc on C_2 of PEP is unknown, but the stereochemistry at C_3 of the tetrahedral adduct derived from FPEP, UDP-GlcNAc, and MurZ in D_2O has been determined (see: Kim, D. H.; Lees, W. J.; Walsh, C. T. *J. Am. Chem. Soc.* **1995**, *117*, 6380–6381).

Scheme 8. Relative Stereochemistry of the Addition and Elimination Steps[47]

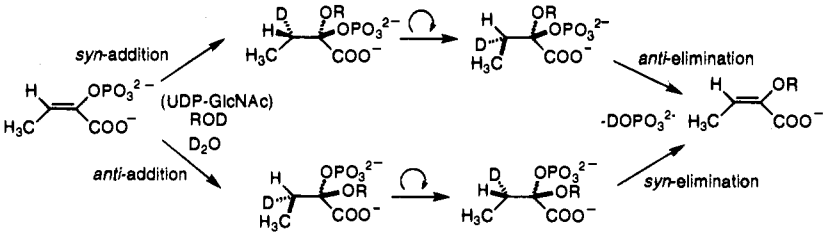

Scheme 9. Proposed Mechanism for MurZ in D_2O with (*E*)-PEB as a Substrate

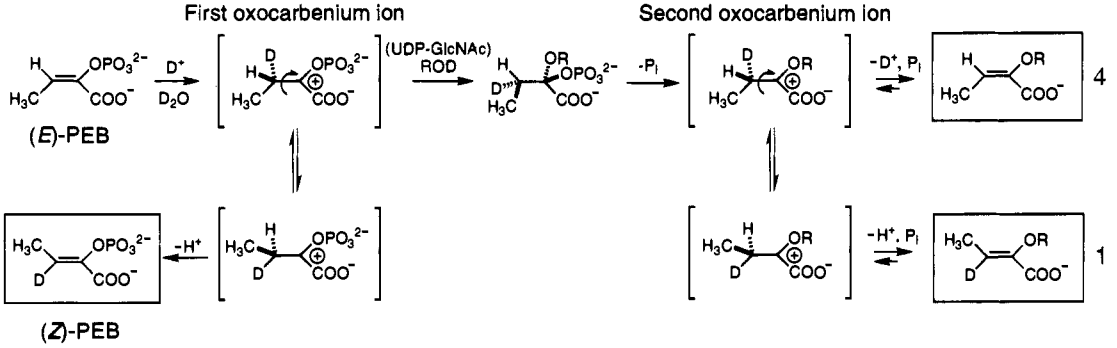

two intermediates that have rotational freedom about their C_2-C_3 bond and that these intermediates must be separated by an energy barrier. We propose that two of the intermediates with rotational freedom about their C_2-C_3 bond are the two oxocarbenium ions because they will be separated by an energy barrier. The partitioning of the first oxocarbenium ion back to (*E*)- and (*Z*)-PEB can be determined from the partitioning of (*E*)-enol ether product to (*E*)- and (*Z*)-PEB, which is 20:1. The partitioning of the first oxocarbenium ion back to (*Z*)-PEB and on to the second oxocarbenium ion can be approximated by the partitioning of (*E*)-PEB to (*Z*)-PEB and products, which is 1:2.6. This latter ratio needs to be adjusted slightly to account for the fact that the second oxocarbenium can partition back to the first oxocarbenium ion without progressing to products. The partitioning of the second oxocarbenium ion in the forward direction to (*E*)- and (*Z*)-enol ether products and back to the first oxocarbenium ion can be determined and approximated in a similar manner and is approximately 13:1:3.

The partitioning of the oxocarbenium ions in H_2O can be used to support the pathway outlined for (*Z*)-PEB in D_2O. In D_2O, (*Z*)-PEB is proposed to be converted to mainly deuterated (*E*)-PEB and then onto deuterated (*E*)- and (*Z*)-enol ether products (Scheme 7). The first oxocarbenium ion generated from (*Z*)-PEB in D_2O will be monodeuterated at C_3, and this oxocarbenium ion should partition to (*E*)-PEB with the loss of a proton or to the second oxocarbenium ion. If this partitioning is the same in D_2O as in H_2O, in which the first oxocarbenium ion also loses a proton to form (*E*)-PEB, then approximately six molecules of deuterated (*E*)-PEB should be generated for every molecule of monodeuterated second oxocarbenium ion. This deuterated (*E*)-PEB will, subsequently, be converted to a dideuterated first oxocarbenium ion and then on to the observed deuterated (*E*)- and (*Z*)-enol ether products as indicated in Scheme 7. Since the monodeuterated second oxocarbenium can also partition back to the first oxocarbenium, the ratio of deuterated to protonated (*Z*)-enol ether product will be greater than 6:1.

Acknowledgment. We thank Dennis H. Kim for his helpful comments. We thank members of the Walsh group for comments on the paper. W. J. L. was supported by a postdoctoral fellowship from the Natural Sciences and Engineering Research Council of Canada. This work was supported in part by National Institutes of Health Grant GM49338-02.

Supporting Information Available: Figures 5–7 indicating the time course of the reaction of (*Z*)-PEB and UDP-GlcNAc and the reaction of (*Z*)-EB-UDP-GlcNAc and phosphate (3 pages). This material is contained in many libraries on microfiche, immediately follows this article in the microfilm version of the journal, can be ordered from the ACS, and can be downloaded from the Internet; see any current masthead page for ordering information and Internet access instructions.

JA950758W